Nonlocal-response diffusion model of holographic recording in photopolymer

John T. Sheridan and Justin R. Lawrence

School of Physics, Faculty of Science, Dublin Institute of Technology, Kevin Street, Dublin 8, Ireland

Received September 13, 1999; accepted January 10, 2000; revised manuscript received March 7, 2000

The standard one-dimensional diffusion equation is extended to include nonlocal temporal and spatial medium responses. How such nonlocal effects arise in a photopolymer is discussed. It is argued that assuming rapid polymer chain growth, any nonlocal temporal response can be dealt with so that the response can be completely understood in terms of a steady-state nonlocal spatial response. The resulting nonlocal diffusion equation is then solved numerically, in low-harmonic approximation, to describe grating formation. The effects of the diffusion rate, the rate of polymerization, and a new parameter, the nonlocal response length, are examined by using the predictions of the model. By applying the two-wave coupled-wave model, assuming a linear relationship between polymerized concentration and index modulation, the resulting variation of the grating diffraction efficiency is examined. © 2000 Optical Society of America [S0740-3232(00)02106-2]

OCIS code: 160.2900.

1. INTRODUCTION

The ability to optically record highly diffraction efficient low-loss volume holographic gratings in self-processing photopolymer materials makes these materials of ever-increasing practical importance.[1] A diffusion-based mechanism of grating formation[2] and a model based on this mechanism of hologram formation have previously been presented in the literature.[3,4] Although this model provides insights into the physical processes taking place, it incorrectly predicts that the higher the spatial frequency recorded, the more ideal the grating recorded.

Several practical reasons can be given for why this theoretical prediction disagrees with experimental results. The recording of high-spatial-frequency gratings requires vibration isolation during exposure. Poor isolation or long exposure times will cause a cumulative smearing of the grating profile. However, it seems reasonable to expect that there is a fundamental physical limit to the minimum grating period recordable that depends on the material's recording mechanism.

In all previous models it is assumed that the response of the photopolymer to the incident light is local; i.e., the effect at a point is independent of effects at all other times and places in the medium. In this paper we discuss the case of a medium in which the response of the material is nonlocal; i.e., the response at point x at time t depends on what happened at a point x' at time t'. Such a nonlocal response can arise from several physical effects, but in particular it may arise from the recording mechanism. In the case of dry photopolymer, gratings are formed when varying numbers of polymer chains are initiated simultaneously in all illuminated areas within the material. The chains then grow away from their initiation point, which leads to a "spreading" of the polymer. We propose that this chain growth is the physical reason for a nonlocal response. Other possible causes such as diffuse scattering of light during recording will not be considered further here.

We now discuss how nonlocal effects might be represented mathematically. Let us assume the isotropic growth of polymer chains outward from any initiation point. We also assume that the length that the chains grow away from their initiation point and the directions of the polymer's bond vectors can be described with a macroscopic distribution function.[5] To represent the spreading of the polymer chains, we introduce two macroscopic probability density functions (PDF's): a chain-length PDF, and a chain-growth velocity PDF, which give the likelihood of a chain having a particular parameter value.

We represent the probability of the existence of a chain of effective length L by

$$P[L] = \exp[-(L - Lm)^2/2\sigma_L]/\sqrt{2\pi\sigma_L}, \tag{1a}$$

and the probability of the existence of a chain growing with velocity v is given by

$$P[v] = \exp[-(v - v_m)^2/2\sigma_v]/\sqrt{2\pi\sigma_v}, \tag{1b}$$

where L_m is the mean effective chain length and σ_L is the chain-length distribution variance while v_m is the mean chain-growth velocity and σ_v the velocity variance. In both cases we assume that the PDF's of the two parameters are well approximated by normal Gaussian distributions.[6] To ensure that nonphysical negative values have very low probabilities of existing, i.e., more than 99% of the total population is positive valued and normally distributed, we assume that $L_m - 2\sqrt{2\sigma_L} > 0$ and $v_m - 2\sqrt{2\sigma_v} > 0$.

Now let us examine the case of two points x and x' separated by a distance $x - x'$ in the recording medium. If $x - x' > L_m + 2\sqrt{2\sigma_L}$, then a negligible number (less than 1%) of chains originating at x' will be of sufficient effective length to reach x. But if $x - x' < L_m - 2\sqrt{2\sigma_L}$, effectively all chains that start to grow at x' will pass through x. In a similar manner we can define effective maximum and minimum velocities. Dividing

the effective maximum connectable separation by the minimum effective velocity, we derive an expression for the maximum effective travel of time $T_{\max}$ between the points.

$$T_{\max} \approx \frac{(x - x')|_{\max}}{v|_{\min}} = \frac{L_m + 2\sqrt{2\sigma_L}}{v_m - 2\sqrt{2\sigma_v}}. \tag{2}$$

The time parameter $T_{\max}$ is of special significance. Given any length of time greater than $T_{\max}$, we are certain that more than 99% of all the chains that started to grow at x' and that are long enough to reach x will have given rise to an amount of polymer at x. In developing our model we assume that over this length of time the monomer concentration at x' varies very little. In this case, following an initial transient period within the system, the cumulative effect of position x' on position x will be instantaneously governed by the amount of polymerization at point x'. If the initiation of chains at position x' changes slowly as a function of time, eventually a steady state is achieved at x. At any time following the initial transient time period $T_{\max}$, all possible x'-initiated polymer chain-length/velocity combinations that can reach the x position will be simultaneously present there. In this way we talk of an average over the time interval $T_{\max}$ to find the accumulative effect of x' on x.

In other words, if chain growth is rapid compared with other temporal effects within the medium, i.e., the rates of monomer diffusion and polymerization, then any change in the time-averaged concentration of monomer at x' will effectively give rise to an *instantaneous* change in the time-averaged amount of polymerization at position x. In this paper we therefore assume that the nonlocal temporal response arising from the growth of the polymer chains can be modeled by using an equivalent instantaneous nonlocal spatial response.

2. NONLOCAL DIFFUSION MODEL

Following the notation of Zhao and Mouroulis,[3] we propose the following extended nonlocal form of the one-dimensional diffusive transport equation for the concentration of monomer $u(x, t)$ in a dry layer:

$$\frac{\partial u(x,t)}{\partial t} = \frac{\partial}{\partial x}\left[D(x,t)\frac{\partial u(x,t)}{\partial x}\right] - \int_{-\infty}^{+\infty}\int_{0}^{t} R(x, x'; t, t') \times F(x', t')u(x', t')\mathrm{d}t'\mathrm{d}x'. \tag{3}$$

In this equation $D(x, t)$ is referred to as the diffusion constant. $F(x', t')$ represents the rate of polymerization [rate of removal of $u(x', t')$] at point x' and time t'. The nonlocal response function $R(x, x'; t, t')$ represents the effect of monomer concentration at location x' and t' on the amount of material being polymerized at location x at time t.

As discussed in the introduction, we argue that averaging takes place over the temporal effects, and we can therefore assume an equivalent instantaneous response. Now, using our introductory arguments regarding time scales, we assume that over the time interval $T_{\max}$ other processes vary little:

$$F(x', t')u(x', t') \approx F(x', t' \pm T_{\max})u(x', t' \pm T_{\max}). \tag{4}$$

Let us assume we can break our nonlocal response function into the product of a spatial and a temporal response: $R(x, x'; t, t') = R(x, x')T(t, t')$. The purely temporal response takes account of the effects of past events over the time interval $0 \leqslant t' < t$. In the local limit the time response function must have the following mathematical property:

$$\lim_{T_{\max}\to 0} [T(t', t)] = \delta(t' - t). \tag{5a}$$

Furthermore, we argue that only events in the recent past, quantified by using $T_{\max}$, will give rise to significant nonlocal temporal effects. The time response must therefore have the properties that

$$\int_{-\infty}^{t} T(t', t)\mathrm{d}t' = 1 \approx \int_{t-T_{\max}}^{t} T(t', t)\mathrm{d}t'. \tag{5b}$$

In expression (5b) the limits of integration indicate that the time response operates only over the range $t - T_{\max} \leqslant t' < t$.

Starting with Eq. (3) and applying Eq. (4) and expression (5b) we argue that

$$\begin{aligned}\int_{0}^{t} R(x, x'; t, t')F(x', t')u(x', t')\mathrm{d}t' &\approx \left[\int_{-T_{\max}}^{t} R(x, x')T(t, t')\mathrm{d}t'\right]F(x', t)u(x', t) \\ &\approx R(x, x')F(x', t)u(x', t).\end{aligned} \tag{6}$$

When these results are combined, diffusion equation (3) becomes

$$\frac{\partial u(x,t)}{\partial t} = \frac{\partial}{\partial x}\left[D(x,t)\frac{\partial u(x,t)}{\partial x}\right] - \int_{-\infty}^{+\infty} R(x, x') \times F(x', t)u(x', t)\mathrm{d}x'. \tag{7a}$$

On examination we see that when the spatial response is local, i.e., $R(x, x') = \delta(x - x')$, we return to the standard one-dimensional diffusion equation for monomer concentration[3,4]:

$$\frac{\partial u(x,t)}{\partial t} = \frac{\partial}{\partial x}\left[D(x,t)\frac{\partial u(x,t)}{\partial x}\right] - F(x,t)u(x,t). \tag{7b}$$

To solve Eq. (7a) we must assume a form for the spatial response function. The response function arises from the growth of chains from the point at which they are initiated into adjacent regions. It will be related to, but not be the same as, the PDF of chain lengths. Furthermore, we assume that the growth of chains will be spatially isotropic, and therefore we expect the response to be an even function of $x - x'$. It would also seem physically reasonable to assume that the probability of a chain initiated at point x' influencing the process at x will decrease as the distance between the two points increases. Finally, as the process approaches the local limit the response function must become a delta function. A mathematical function that satisfies all these criteria is

$$R(x - x') = \frac{\exp[-(x - x')^2/2\sigma]}{\sqrt{2\pi\sigma}}, \tag{8a}$$

where we refer to the square root of the variance $\sqrt{\sigma}$ as the nonlocal response length since it characterizes the length scale over which the nonlocal effect is significant. We note that

$$\lim_{\sigma\to 0}\frac{\exp[-(x - x')^2/2\sigma]}{\sqrt{2\pi\sigma}} = \delta(x - x'),$$

$$\int_{-\infty}^{+\infty}\frac{\exp[-(x - x')^2/2\sigma]}{\sqrt{2\pi\sigma}}\mathrm{d}x' = 1. \tag{8b}$$

Equation (7a) is now solved; we have closely followed the method of Zhao and Mouroulis[3] with the nonlocal response presented in Eq. (8a), given the initial condition $u(x, 0) = 100$ for $-\infty < x < +\infty$. Following Ref. 3 we assume a recording intensity of the form

$$I(x, t) = I_0[1 + V\cos(Kx)], \tag{9a}$$

where I_0 is the average intensity in the medium, V is the fringe visibility, $K = 2\pi/\Lambda$ is the grating spatial frequency, and Λ is the resulting grating period. We assume that the rate of polymerization is directly proportional to the exposing intensity, and therefore

$$F(x, t) = F_0[1 + V\cos(Kx)], \tag{9b}$$

where $F_0 = \kappa I_0$, κ a fixed constant. The monomer concentration is written as a four-harmonic expansion,

$$u(x, t) = \sum_{l=0}^{M=3} u_i(t)\cos(iKx), \tag{10}$$

and the diffusion constant is expanded in a two-harmonic expansion,

$$D(x, t) = \sum_{i=0}^{M=1} D_i(t)\cos(iKx). \tag{11}$$

When these expansions are substituted into Eq. (7a), the following set of first-order coupled concentration equations can be derived:

$$\frac{\mathrm{d}u_0(\xi)}{\mathrm{d}\xi} = -u_0(\xi) - \frac{V}{2}u_1(\xi), \tag{12a}$$

$$\frac{\mathrm{d}u_1(\xi)}{\mathrm{d}\xi} = -V\exp(-K^2\sigma/2)u_0(t) - [\exp(-K^2\sigma/2) + R\exp(-\alpha\xi)\cosh(\alpha V\xi)]u_1(\xi) - \left[\frac{V}{2}\exp(-K^2\sigma/2) + R\exp(-\alpha\xi)\sinh(\alpha V\xi)\right]u_2(\xi), \tag{12b}$$

$$\frac{\mathrm{d}u_2(\xi)}{\mathrm{d}\xi} = -\{\exp[-(2K)^2\sigma/2] + 4R\exp(-\alpha\xi)\cosh(\alpha V\xi)\}u_2(\xi) - \left\{\frac{V}{2}\exp[-(2K)^2\sigma/2] - R\exp(-\alpha\xi)\sinh(\alpha V\xi)\right\}u_1(\xi) - \left\{\frac{V}{2}\exp[-(2K)^2\sigma/2] - 3R\exp(-\alpha\xi)\sinh(\alpha V\xi)\right\}u_3(\xi), \tag{12c}$$

$$\frac{\mathrm{d}u_3(\xi)}{\mathrm{d}\xi} = -\{\exp[-(3K)^2\sigma/2] + 9R\exp(-\alpha\xi)\cosh(\alpha V\xi)\}u_3(\xi) - \left\{\frac{V}{2}\exp[-(3K)^2\sigma/2] + 3R\exp(-\alpha\xi)\sinh(\alpha V\xi)\right\}u_2(\xi), \tag{12d}$$

where u_0, u_1, u_2 and u_3 are the first four monomer-concentration harmonics, σ is the nonlocal variance, and α is a constant that characterizes the rate of decrease of the diffusion coefficients; see Ref. 3. $R = DK^2/F_0$ is the ratio of the diffusion rate and the polymerization rate, and $\xi = F_0 t = \kappa I_0 t$ is the illumination time t multiplied by irradiance.

The resulting concentration of polymerized monomer, after an exposure of duration t seconds, is given by a modified version of the driving function of Eq. (7a),[3]

$$N(x, t) = \int_0^t\int_{-\infty}^{+\infty} R(x - x')F(x', t'')u(x', t'')\mathrm{d}x'\mathrm{d}t'', \tag{13}$$

giving the following polymerization-concentration spatial-harmonic components:

$$N_0(\xi) = \int_0^{\xi}[u_0(\xi'') + (V/2)u_1(\xi'')]\mathrm{d}\xi'', \tag{14a}$$

$$N_1(\xi) = \exp(-K^2\sigma/2)\int_0^{\xi}[Vu_0(\xi'') + u_1(\xi'') + (V/2)u_2(\xi'')]\mathrm{d}\xi'', \tag{14b}$$

$$N_2(\xi) = \exp[-(2K)^2\sigma/2]\int_0^{\xi}[(V/2)u_1(\xi'') + u_2(\xi'') + (V/2)u_3(\xi'') +]\mathrm{d}\xi'', \tag{14c}$$

$$N_3(\xi) = \exp[-(3K)^2\sigma/2]\int_0^{\xi}[(V/2)u_2(\xi'') + u_3(\xi'')]\mathrm{d}\xi''. \tag{14d}$$

It is now assumed that the modulation of the refractive index induced during recording is approximately linearly related to the polymer concentration. Therefore each of the above terms corresponds to a change in the size of a spatial-frequency component of a grating pattern recorded in the volume:

$$n(x, \xi) = n_{\mathrm{av}} + C \sum_{i=0}^{M=3} N_i(\xi)\cos(iKx). \qquad (15)$$

3. NUMERICAL RESULTS

We wish to explore changes to the local response diffusion model predictions, which arise from the introduction of the nonlocal response. We do this by carrying out a set of calculations for the local response case,[3,4] and then comparing these with the corresponding nonlocal predictions. Three values of σ are used in the following calculations: $\sigma = 0$ (local case), $\sigma = 1/64$, and $\sigma = 1/32$. For generality we normalize all length scales with respect to the grating period length. The values of variance correspond to the square of a length within the grating. A variance of $\sigma = 1/64$ corresponds, in the grating material, to a response-length scale of one eighth of a period and indicates the length range over which the effects of a point

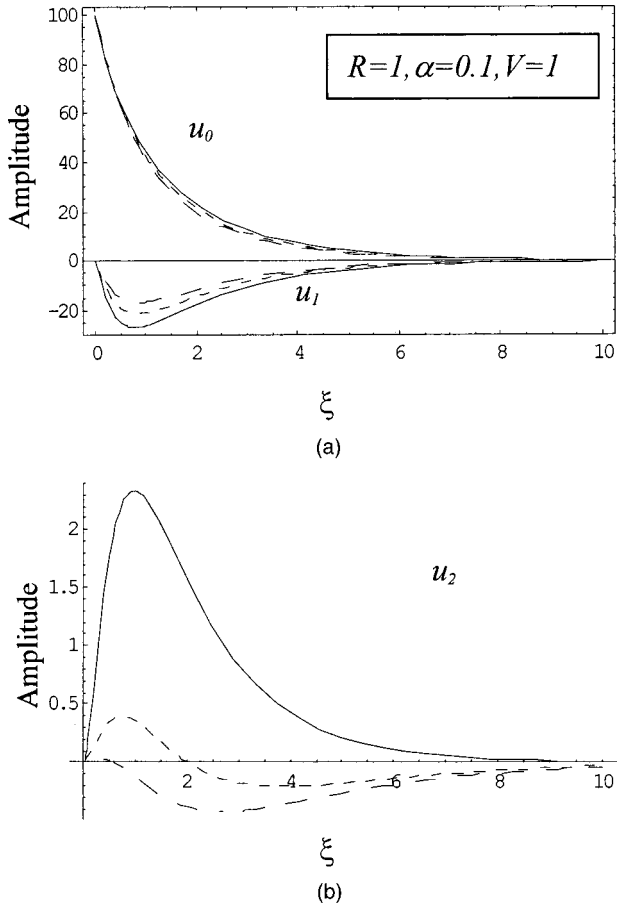

Fig. 1. Monomer-concentration amplitudes: (a) u_0 and u_1, (b) u_2 versus exposure ξ. Solid curves, $\sigma = 0$; short-dashed curves $\sigma = 1/64$; long-dashed curves, $\sigma = 1/32$.

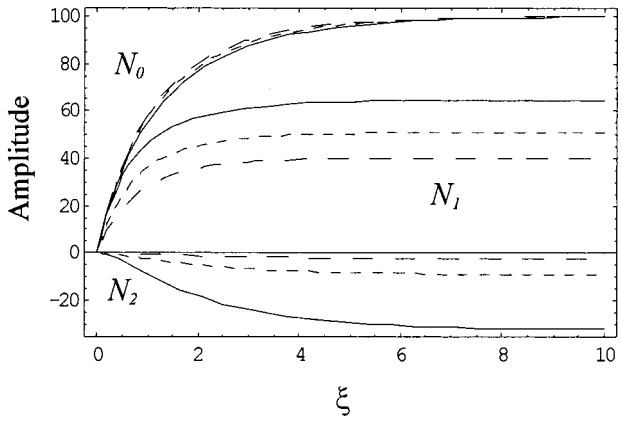

Fig. 2. Polymer-concentration amplitudes versus ξ for $R = 1$. Solid curves, $\sigma = 0$; short-dashed curves $\sigma = 1/64$; long-dashed curves, $\sigma = 1/32$.

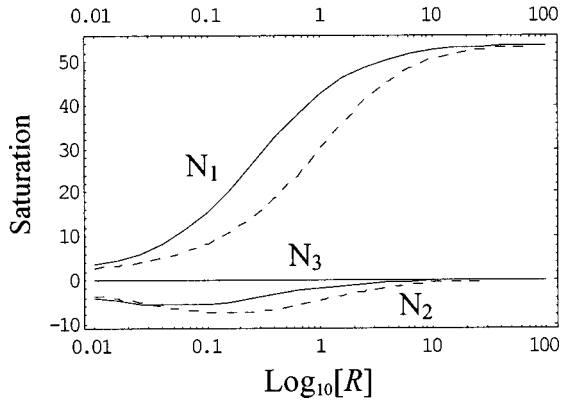

Fig. 3. Saturation values, $\xi = 40$, of the first three harmonics of polymer concentration as functions of $\log_{10} R$. Nonlocal response variance, $\sigma = 1/32$. In all cases $V = 1$. Solid curves, $\alpha = 0$; dashed curves $\alpha = 1$.

are significant. The reason these values of variance were chosen was that they were found to provide clearly visible and typical results.

Equations (12) and (14) are solved numerically with Mathematica[7] run on a personal computer. Using the four-harmonic expansion of the monomer concentration, we first calculate the harmonic amplitudes over the range $0 \leqslant \xi \leqslant 10$ for the case where $V = 1$, $\alpha = 0.1$, and $R = 1$ (Fig. 1). In Fig. 1(a) the variation of the amplitudes of the zeroth, u_0, and first, u_1, harmonics as functions of exposure energy ξ are presented. In each case the curves for three values of nonlocal variance are presented: $\sigma = 0$ (local case), $\sigma = 1/64$, and $\sigma = 1/32$. The corresponding graph for the second-order monomer-concentration harmonic are shown in Fig. 1(b). The amplitudes of all the monomer harmonics are seen to decrease with time; also, the larger the value of σ, the more rapidly the monomer is polymerized. The corresponding harmonics of polymer concentration are shown in Fig. 2. The effect of σ is to decrease the saturation levels of the higher-order harmonics, thereby decreasing the amplitude but improving the sinusoidal purity of the profile shape.

Taking the case where $\sigma = 1/32$, we follow Zhao and Mouralis[3] and plot the variations of the saturation values (calculated for $\xi = 40$) of the first three harmonics of the polymer profile as a function of $\log_{10} R$. The saturation values are presented in Fig. 3 for the cases where $\alpha = 0$ (solid curves) and where $\alpha = 1$ (dashed curves). In agreement with Zhao and Mouroulis, we find that α simply introduces a shift of the curves to the right, implying that only the zeroth-order diffusion component D_0 must be retained. Most noticeably, as σ increases from zero (see Ref. 3), the saturation value of N_1 decreases. Both the second- and third-order harmonics also have smaller maximum values and decrease more rapidly as a function of R.

The effects of varying the illuminating fringe visibility V on the saturated amplitude of N_1 has also been examined for various nonzero, nonlocal variances. When $R > 25$ the response for all three values of σ (0, 1/64, 1/32) is linear, with decreasing maximum N_1 as σ increases. As R decreases in size and σ increases, the relationship $N_1(V)$ becomes less linear and N_1 decreases rapidly in amplitude.

4. GRATING PROFILES AND DIFFRACTION EFFICIENCIES

We have now examined the amplitudes of both the monomer and the resulting polymer-concentration harmonics. In Fig. 4 we present a set of three polymer-concentration profiles, following an exposure of $\xi = 20$, plotted over one grating period, with $V = 1$ and $\alpha = 0.1$. In Fig. 4(a) $R = 1$, in Fig. 4(b) $R = 50$, and in Fig. 4(c) $R = 0.05$. In each case the profiles for values of $\sigma = 0$, 1/64, and 1/32 are presented. We note that the results in Fig. 4(a) correspond to the cases examined in Figs. 1 and 2.

In Fig. 4(a) ($R = 1$), there is significant distortion in the local response profile recorded. Increasing the nonlocal variance smoothes the profile, and while the profile visibility decreases, its harmonic purity increases. When $R = 50$ [Fig. 4(b)], the largest and purest sinusoidal grating profiles are achieved. Increasing σ decreases the profile visibility. In Fig. 4(c) ($R = 0.05$), the most-nonlinear profiles with the lowest visibility occur. Once again, increasing σ smoothes the profile, thus decreasing the profile visibility.

As stated in Section 2, we assume that a linear relationship exists between the strength of the refractive-index changes that occur in the material and the strength of the polymer concentration. The first-order, two-wave coupled-wave model[8] predicts that the diffraction efficiency of a volume unslanted transmission phase grating replayed at the Bragg condition is given by

$$\eta = \sin^2\left(\frac{\pi \Delta n d}{\lambda \cos\theta}\right), \tag{16a}$$

where d is the grating thickness, λ the replay wavelength, θ the replay angle and Δn the amplitude of the first-order refractive-index modulation harmonic. This model assumes that the effects of all higher-order-grating spatial components can be neglected.[9] Typical values of these parameters are $d = 100\,\mu$m, $\lambda = 500$ nm, $\theta = 30°$,

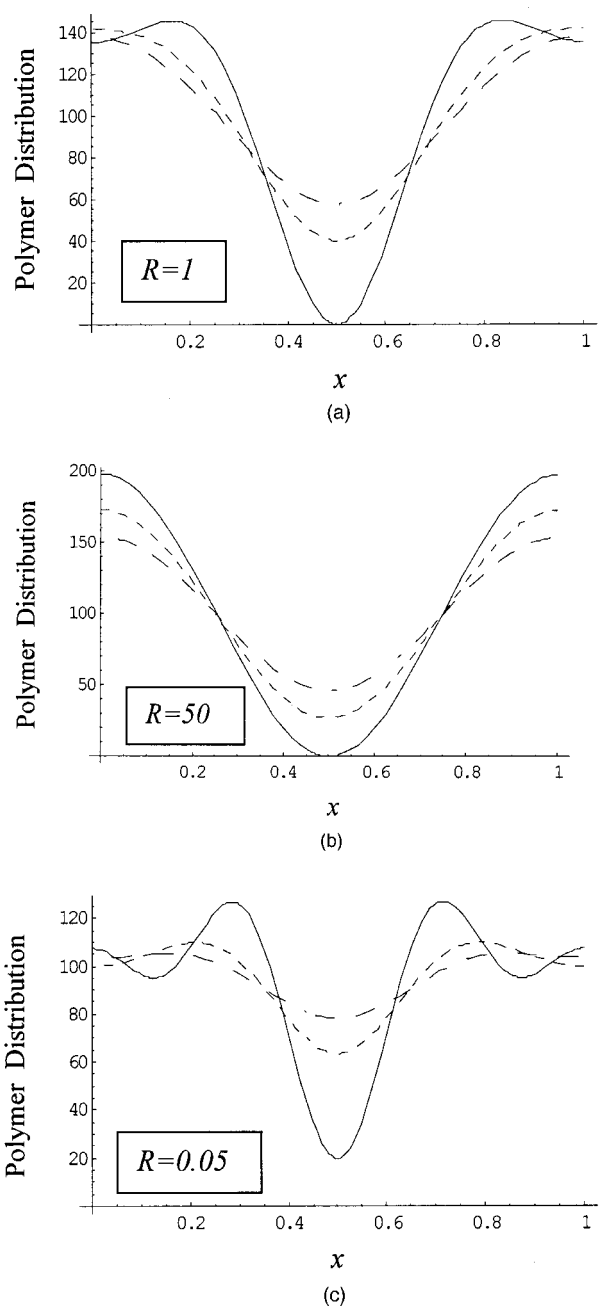

Fig. 4. Spatial distribution profiles of polymer concentrations: (a) $R = 1$, (b) $R = 50$, (c) $R = 0.05$; In all cases $V = 1$ and $\alpha = 0.1$. Nonlocal variances: solid curves, $\sigma = 0$; short-dashed curves $\sigma = 1/64$; long-dashed curves, $\sigma = 1/32$.

which will produce a grating of period $\Lambda = \lambda/(2 \sin\theta) = 500$ nm. We assume that $\Delta n = CN_1(\xi)$ and that therefore

$$\eta(\xi) \approx \sin^2[725.5 \times CN_1(\xi)]. \tag{16b}$$

Given that a value of Δn of ~0.002 will provide a diffraction efficiency close to 100%, when we examine our results for N_1 it can be seen that a value of $C \approx 4.3 \times 10^{-5}$ will provide an experimentally achievable diffraction-efficiency result.

Using these parameter values we present the diffraction-efficiency growth curves in Figs. 5(a), 5(b), and

5(c) for the same three sets of grating profiles shown in Figs. 4(a), 4(b), and 4(c), respectively. The diffraction efficiency is shown as a function of ξ (exposure energy). From the model we expect an increase in diffraction efficiency up to a maximum value of 1, or 100%, followed by overmodulation.

From Figs. 5(a)–5(c) we see that both R and σ have very strong effects on the diffraction efficiency of the grating. In general the larger R, the faster the growth of the grating and the higher the modulation achievable. Increasing the nonlocal variance acts to slow down the growth of the diffraction efficiency and to reduce the maximum saturation modulation achievable.

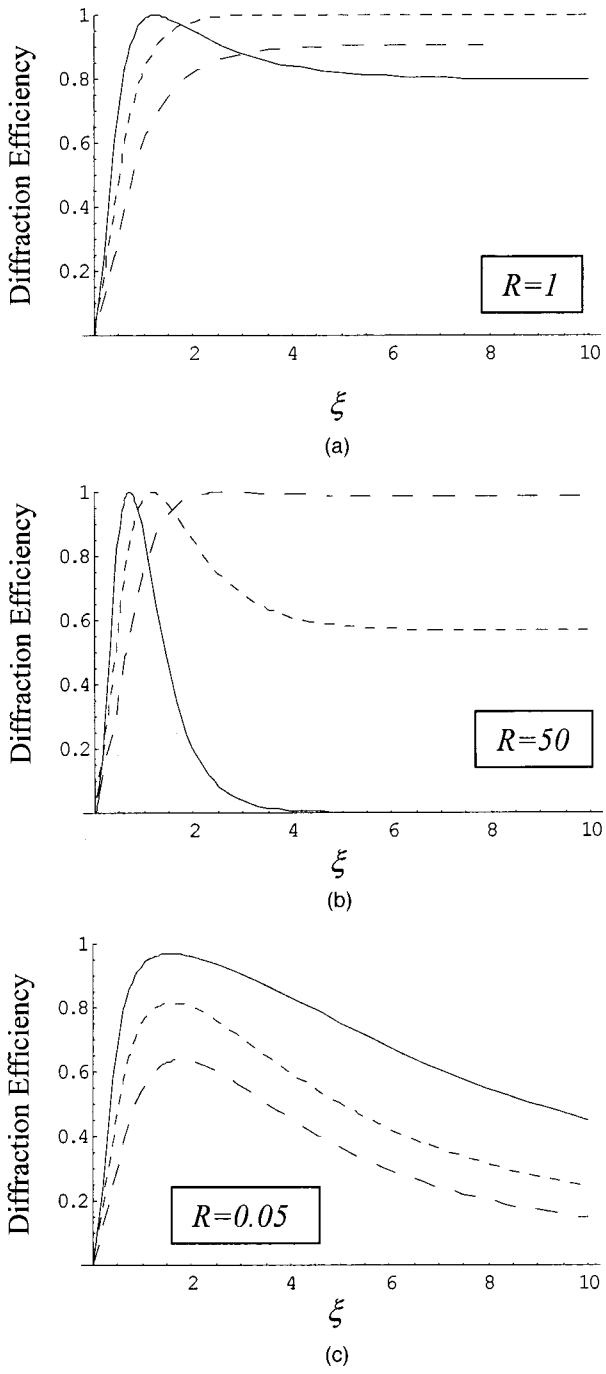

Fig. 5. First-order, two-wave coupled-wave model prediction of the diffraction-efficiency growth curves of the gratings for the polymer-concentration profiles shown in Fig. 4: (a) $R = 1$, (b) $R = 50$, (c) $R = 0.05$; $V = 1$ and $\alpha = 0.1$. Nonlocal variances: solid curves, $\sigma = 0$; short-dashed curves, $\sigma = 1/64$; long-dashed curves, $\sigma = 1/32$.

5. CONCLUSIONS

The nonlinear diffusion model for hologram formation in photopolymer has been extended to include nonlocal spatial response effects. To do so we have assumed that nonlocal temporal effects occur on a short time scale, which allows them to be treated as effectively instantaneous.

The predictions of the local diffusion model, $\sigma = 0$, (Refs. 3 and 4) might be stated as follows. In general the larger the value of R, the stronger the first-order grating and the more closely the resulting grating profile matches the illuminating fringe pattern. We can summarize these results as follows:

1. As I_0 increases, F_0 increases and R decreases.
2. As Λ increases, K decreases and R decreases.

Therefore the lower the illuminating intensity (the longer the exposure) and the finer the fringe period, the larger R and so the better the profile.

In the nonlocal response regime, $\sigma > 0$, a further qualification must be noted. The larger the nonlocal response variance, the lower the visibility of the profile but also the more closely the profile recorded resembles the sinusoidal interference pattern. Experimentally, one usually works with a fixed material in which the chain-length and chain-growth velocity PDF's are fixed. As the recording fringe-pattern period decreases, the ratio of the nonlocal response variance to the period squared increases. In this situation eventually the grating amplitude is so weak as to be negligible. Therefore we have two additional predicted results:

3. As Λ decreases, $K^2\sigma$ increases, $\Delta n = CN_1$ decreases, and the first-order grating is suppressed.
4. As Λ decreases, $(mK)^2\sigma$ increases more rapidly, and so $\Delta n_m = CN_m$ decreases and the higher-order-grating harmonics are even more heavily suppressed.

Here N_m is the mth-order polymer-concentration harmonic.

The diffusion model has been extended in a way that should make it applicable to a wider range of observable phenomena. This simple monomer diffusion and polymerization model is insufficient to explain all aspects of hologram formation. For example, the diffusion of dye molecules also affects the process. A model of much greater complexity may be required to predict the material behavior fully.

ACKNOWLEDGMENT

The authors acknowledge the assistance provided by the Dublin Institute of Technology's Strategic Research and Development program.

The authors can be reached at the address on the title page or by e-mail: john.sheridan@dit.ie and justin.lawrence@dit.ie.

REFERENCES

1. G. Manivannan and R. A. Lesard, "Trends in holographic recording materials," Trends Polym. Sci. **2**, 282–290 (1994).
2. W. S. Colburn and K. A. Haines, "Volume hologram formation in photopolymer materials," Appl. Opt. **10**, 1636–1641 (1971).
3. G. Zhao and P. Mouroulis, "Diffusion model of hologram formation in dry photopolymer materials," J. Mod. Opt. **41**, 1929–1939 (1994).
4. V. L. Colvin, R. G. Larson, A. L. Harris, and M. L. Schilling, "Quantitative model of volume hologram formation in photopolymers," J. Appl. Phys. **81**, 5913–5923 (1997).
5. M. Doi, *Introduction to Polymer Physics* (Clarendon, Oxford, UK, 1997), pp. 1–8.
6. H.-G. Elias, *Macromolecules, Part I. Structures and Properties* (Plenum, New York, 1977), p. 151.
7. S. Wolfram, *Mathematica*, 3rd ed. (Cambridge U. Press, Cambridge, UK, 1996).
8. H. Kogelnik, "Coupled wave theory for thick holographic gratings," Bell Syst. Tech. J. **48**, 2909–2947 (1969).
9. R. R. A. Syms, *Practical Volume Holography* (Clarendon, Oxford, UK, 1990).